Journal of the Optical Society of Korea, Vol. 11, No. 1, March 2007, pp. 10-17

Phase Error due to Polarization Components of the Modified Triangular Interferometer

Soo-Gil Kim*

Information & Control Eng., Hoseo Univ., San 29-1, Sechul-ri, Baebang-myun, Asan-city, Choongnam, 336-795, Korea

(Received December 21, 2006 : revised February 5, 2007)

We need two operation modes to obtain the complex hologram without bias and the conjugate image in the modified triangular interferometer (MTI). To solve the problem, we proposed the optimized MTI with one wave plate, which can obtain cosine and sine functions by the combination of one wave plate and one linear polarizer. In the extraction of phase term using the combination of polarization components, the phase error occurs, and we analyzed such potential phase errors in the optimized MTI.

OCIS codes : 090.2870, 090.2880

I. INTRODUCTION

Incoherent imaging system is usually limited in image processing due to the nonnegative point-spread function (PSF) [1]. By employing a two-pupil system, such limitations can be overcomed [2,3]. The pupils are created by either amplitude or wave-front divisions [3-5]. Any bipolar impulse response can be synthesized by using two-pupil methods. The synthesis methods are classified into nonpupil interaction synthesis and pupil interaction synthesis [2]. Two-pupil systems are usually implemented by separating the interactive term and the noninteractive term on the basis of the spatial or temporal carriers [4-6].

In previous our works, two-pupil synthesis by the MTI, which is an incoherent hologram formation system, was reported [7,8]. A simple two-pupil interaction system was implemented by adding two wave plates and a linear polarizer to Cochran's triangular interferometer [9].

In this paper, we introduce two-pupil synthesis of OTF in the MTI, and then we demonstrate that removal of bias and conjugate image of the incoherent hologram is possible through two-pupil synthesis, and we present the optimal MTI, which can obtain any bipolar function by combining a wave plate and a linear polarizer.

The phase term of complex hologram in the MTI is obtained from four intensity patterns by phase-shifting technique. A phase shift or modulation in the phase-shifting techniques can be induced by moving a mirror, tilting a glass plate, moving a grating, rotating a half-wave plate or analyzer [10-13].

In the MTI, a phase shift is implemented by the combination of phase retardation and rotation angle of polarization components such as a wave plate and a linear polarizer. In the extraction of phase term using the combination of polarization components, the phase error occurs. In this paper, we analyze its potential error sources caused by polarization components.

II. TWO-PUPIL SYNTHESIS OF OTF OF THE MTI

A. One-pupil synthesis of the MTI

Figure 1 shows the MTI obtained by modification of the triangular interferometer. In Fig. 1, PBS represents a polarizing beam splitter. Lens1 and lens2 are lenses with focal lengths f_1 and f_2, respectively. Linear polarizer is x polarized. If a linear polarizer and wave plates are removed and the PBS is replaced with an ordinary beam splitter, the system is the same as Cochran's triangular interferometer [9]. And, the impulse response functions of the light that travels clockwise and counterclockwise in the Cochran's triangular interferometer, respectively, are given by[7]

$$p_{cw}(x,y)=i\frac{k}{2\sqrt{2}\pi z_0}\exp\left\{-i\frac{k}{2z_0}\left[(\alpha x-x_0)^2+(\alpha y-y_0)^2\right]\right\}=a\exp(-i\theta_{cw}), \tag{1}$$

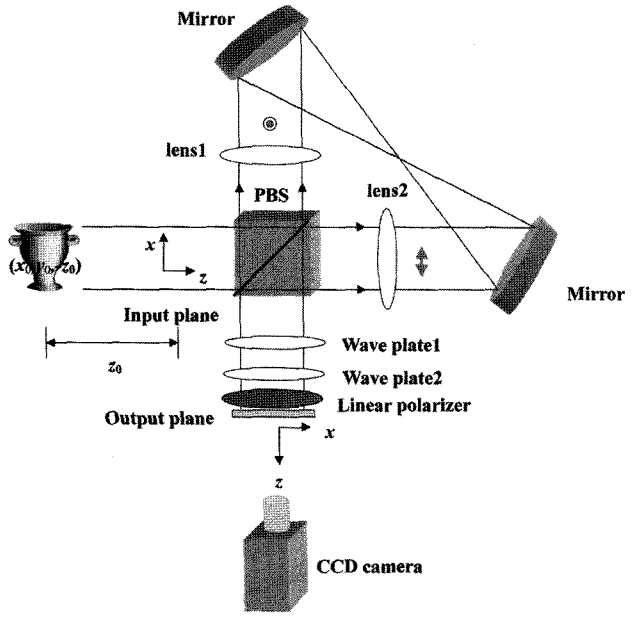

FIG. 1. Modified triangular interferometer.

$$p_{ccw}(x,y)=i\frac{k}{2\sqrt{2}\pi z_0}\exp\left\{-i\frac{k}{2z_0}\left[(\beta x-x_0)^2+(\beta y-y_0)^2\right]\right\}=b\exp(-i\theta_{ccw}), \tag{2}$$

where k is the wave number, z_0 is the distance from the object to the input plane, and $\alpha\equiv-f_1/f_2$, $\beta\equiv-f_2/f_1$.

The polarizations of the light that travels clockwise and counterclockwise are vertical and horizontal, respectively. Using Jones vector representation [14], the impulse response functions of the light that travels clockwise and counterclockwise in one-pupil system of Fig. 1, respectively, are given by

$$p_{mcw}=P_xR(-\psi)W_2R(\psi)R(-\psi)W_1R(\psi)p_{cw}=W_{mcw}p_{cw}, \tag{3}$$

$$p_{mccw}=P_xR(-\psi)W_2R(\psi)R(-\psi)W_1R(\psi)p_{ccw}=W_{mccw}p_{ccw}, \tag{4}$$

where P_x, $R(\psi)$, W_1, and W_2 are defined as

$$P_x=\begin{pmatrix}1&0\\0&0\end{pmatrix},$$

$$R(\psi)=\begin{pmatrix}\cos\psi&\sin\psi\\-\sin\psi&\cos\psi\end{pmatrix},$$

$$W_1=\exp(-i\phi)\begin{pmatrix}\exp(-i\Gamma_1/2)&0\\0&\exp(i\Gamma_1/2)\end{pmatrix},$$

$$W_2=\exp(-i\phi)\begin{pmatrix}\exp(-i\Gamma_2/2)&0\\0&\exp(i\Gamma_2/2)\end{pmatrix},$$

$$\phi=\frac{1}{2}(n_s+n_f)\frac{\omega l}{c},$$

where P_x represents Jones matrix of a linear polarizer, ψ represents the azimuth angle of slow axis of a wave plate with respect to the x axis. Γ_1 and Γ_2 represent the phase retardations of wave plates 1 and 2, respectively. n_s and n_f represent the refractive index of the slow and fast components of wave plates, respectively, and ω, l, c represent the frequency of the light beam, the thickness of wave plate, and the velocity of the light in the vacuum, respectively.

Then, the pupil functions of upper arm and lower arm in Fig. 2 are given by, respectively,

$$P_{mcw}(f_x,f_y)=-i\exp(i\frac{\Gamma_1}{2})\sin\frac{\Gamma_2}{2}P_{cw}(f_x,f_y), \tag{5}$$

$$P_{mccw}(f_x,f_y)=\exp(-i\frac{\Gamma_1}{2})\cos\frac{\Gamma_2}{2}P_{ccw}(f_x,f_y). \tag{6}$$

Because for incoherent imaging systems, the OTF is simply the autocorrelation of the pupil function of the system [15], the OTFs corresponding to Eqs. (5) and (6) are given by

$$OTF_{mcw}=P_{mcw}(f_x,f_y)\otimes P_{mcw}(f_x,f_y), \tag{7}$$

$$OTF_{mccw}=P_{mccw}(f_x,f_y)\otimes P_{mccw}(f_x,f_y), \tag{8}$$

where $\otimes$ denotes the correlation operation, and f_x and f_y denote the spatial frequencies., Because the autocorrelation of any function has central maximum, we see that any bipolar function cannot be produced by the one-pupil system of the MTI.

B. Two-pupil synthesis of the MTI

We describe the OTF of the MTI based on two-pupil synthesis [2]. We add P_{mcw} to P_{mccw} in order to produce an effective pupil function. Then, the effective pupil function for the MTI in Fig. 1 is given by

$$\begin{aligned}P(f_x,f_y)&=P_{mcw}+P_{mccw}\\&=\exp(-i\frac{\Gamma_1}{2})\left[\cos\frac{\Gamma_2}{2}P_{ccw}(f_x,f_y)-i\exp(i\Gamma_1)\sin\frac{\Gamma_2}{2}P_{cw}(f_x,f_y)\right].\end{aligned} \tag{9}$$

In the case of the incoherent system, the OTF of Eq. (9) is given by

$$\begin{aligned}OTF&=P(f_x,f_y)\otimes P(f_x,f_y)\\&=\cos^2\frac{\Gamma_2}{2}P_{ccw}(f_x,f_y)\otimes P_{ccw}(f_x,f_y)+\sin^2\frac{\Gamma_2}{2}P_{cw}(f_x,f_y)\otimes P_{cw}(f_x,f_y)\\&+i\exp(-i\Gamma_1)\cos\frac{\Gamma_2}{2}\sin\frac{\Gamma_2}{2}P_{ccw}(f_x,f_y)\otimes P_{cw}(f_x,f_y)\\&-i\exp(i\Gamma_1)\cos\frac{\Gamma_2}{2}\sin\frac{\Gamma_2}{2}P_{cw}(f_x,f_y)\otimes P_{ccw}(f_x,f_y).\end{aligned} \tag{10}$$

The PSF corresponding to Eq. (10) is given by

$$h(x,y;\Gamma_1,\Gamma_2)=\cos^2\frac{\Gamma_2}{2}|p_{ccw}(x,y)|^2+\sin^2\frac{\Gamma_2}{2}|p_{cw}(x,y)|^2 +i\exp(-i\Gamma_1)\cos\frac{\Gamma_2}{2}\sin\frac{\Gamma_2}{2}p_{ccw}(x,y)p_{cw}^{*}(x,y) -i\exp(i\Gamma_1)\cos\frac{\Gamma_2}{2}\sin\frac{\Gamma_2}{2}p_{cw}(x,y)p_{ccw}^{*}(x,y). \quad (11)$$

We synthesize the PSFs to produce the complex hologram without bias and the conjugate image. A desired PSF is obtained by subtracting the PSFs of two different filter functions obtained from two-pupil synthesis method.

First, in the case in which $\Gamma_1 = \pi/2$ and $\Gamma_2 = \pm\pi/2$, from Eq. (11), we obtain the cosine component.

$$h_r(x,y)=\frac{1}{2}\left[h(x,y;\frac{\pi}{2},\frac{\pi}{2})-h(x,y;\frac{\pi}{2},-\frac{\pi}{2})\right] =|p_{cw}(x,y)p_{ccw}(x,y)|\cos\phi(x,y), \quad (12)$$

where $\phi(x, y) = \theta_{cw}(x, y) - \theta_{ccw}(x, y)$ is the phase difference of the optical waves that travel clockwise and counterclockwise.

And, in the case in which $\Gamma_1 = 0$ and $\Gamma_2 = \pm\pi/2$, from Eq. (11), we obtain the sine component.

$$h_i(x,y)=\frac{1}{2}\left[h(x,y;0,-\frac{\pi}{2})-h(x,y;0,\frac{\pi}{2})\right] =|p_{cw}(x,y)p_{ccw}(x,y)|\sin\phi(x,y). \quad (13)$$

We obtain the synthesized impulse response function using Eqs. (12) and (13). It is described as follows.

$$H(x,y)=|p_{cw}(x,y)p_{ccw}(x,y)|[\cos\phi(x,y)\pm i\sin\phi(x,y)] =|p_{cw}(x,y)p_{ccw}(x,y)|\exp[\pm i\phi(x,y)] \quad (14)$$

The synthesized impulse response function using the two-pupil synthesis method is equivalent to the complex hologram without bias and the conjugate image[7].

C. The optimization of the MTI

In Section B, we can obtain the complex hologram without bias and without conjugate image by the combination of the phase retardation of wave plates in the MTI. However, to obtain the sine function, we use the intensity patterns obtained using the MTI that wave plate 1 is removed. That means that we need two operation modes to obtain the complex hologram without bias and conjugate image in the MTI. In other words, in obtaining the complex hologram, we use two wave plates to obtain the cosine function, and use one wave plate to obtain the sine function in the MTI. Two operation modes are inconvenient in the case of using the MTI. Accordingly, to solve the problem, we need to obtain the cosine function in the MTI that wave plate 1 is removed. The method of obtaining the cosine function using only wave plate 2 is described in the following.

Based on two-pupil synthesis, the effective pupil function of the MTI with a linear polarizer oriented at an azimuth of 45 degrees in Fig. 1 is given by

$$P_{45}(f_x,f_y)=\frac{1}{2}\exp(-i\frac{\Gamma_1}{2})\left\{\left[(\cos\frac{\Gamma_2}{2}-i\sin\frac{\Gamma_2}{2})P_{ccw}(f_x,f_y)+\exp(i\Gamma_1)(\cos\frac{\Gamma_2}{2}-i\sin\frac{\Gamma_2}{2})P_{cw}(f_x,f_y)\right]\hat{x} +\left[(\cos\frac{\Gamma_2}{2}-i\sin\frac{\Gamma_2}{2})P_{ccw}(f_x,f_y)+\exp(i\Gamma_1)(\cos\frac{\Gamma_2}{2}-i\sin\frac{\Gamma_2}{2})P_{cw}(f_x,f_y)\right]\hat{y}\right\}. \quad (15)$$

In the case of the incoherent system, the OTF of Eq. (15) is given by

$$OTF=\frac{1}{2}(\cos^2\frac{\Gamma_2}{2}+\sin^2\frac{\Gamma_2}{2})[P_{ccw}(f_x,f_y)\otimes P_{ccw}(f_x,f_y)+P_{cw}(f_x,f_y)\otimes P_{cw}(f_x,f_y) +\exp(-i\Gamma_1)P_{ccw}(f_x,f_y)\otimes P_{cw}(f_x,f_y)+\exp(i\Gamma_1)P_{cw}(f_x,f_y)\otimes P_{ccw}(f_x,f_y)]. \quad (16)$$

The PSF corresponding to Eq. (16) is given by

$$h_{45}(x,y;\Gamma_1,\Gamma_2)=\frac{1}{2}(\cos^2\frac{\Gamma_2}{2}+\sin^2\frac{\Gamma_2}{2})[|p_{ccw}(x,y)|^2+|p_{cw}(x,y)|^2 +\exp(-i\Gamma_1)p_{ccw}(x,y)p^{*}_{cw}(x,y)+\exp(i\Gamma_1)p_{cw}(x,y)p^{*}_{ccw}(x,y)]. \quad (17)$$

By the same method as before, the effective pupil function of the MTI with a linear polarizer oriented at an azimuth of -45 degree in Fig. 1 is given by

$$P_{-45}(f_x,f_y)=\frac{1}{2}\exp(-i\frac{\Gamma_1}{2})\left\{\left[(\cos\frac{\Gamma_2}{2}+i\sin\frac{\Gamma_2}{2})P_{ccw}(f_x,f_y)-\exp(i\Gamma_1)(\cos\frac{\Gamma_2}{2}+i\sin\frac{\Gamma_2}{2})P_{cw}(f_x,f_y)\right]\hat{x} +\left[-(\cos\frac{\Gamma_2}{2}+i\sin\frac{\Gamma_2}{2})P_{ccw}(f_x,f_y)+\exp(i\Gamma_1)(\cos\frac{\Gamma_2}{2}+i\sin\frac{\Gamma_2}{2})P_{cw}(f_x,f_y)\right]\hat{y}\right\}. \quad (18)$$

In the case of the incoherent system, the OTF of Eq. (18) is given by

$$OTF=\frac{1}{2}(\cos^2\frac{\Gamma_2}{2}+\sin^2\frac{\Gamma_2}{2})[P_{ccw}(f_x,f_y)\otimes P_{ccw}(f_x,f_y)+P_{cw}(f_x,f_y)\otimes P_{cw}(f_x,f_y) -\exp(-i\Gamma_1)P_{ccw}(f_x,f_y)\otimes P_{cw}(f_x,f_y)-\exp(i\Gamma_1)P_{cw}(f_x,f_y)\otimes P_{ccw}(f_x,f_y)]. \quad (19)$$

The PSF corresponding to Eq. (19) is given by

$$h_{-45}(x,y;\Gamma_1,\Gamma_2)=\frac{1}{2}(\cos^2\frac{\Gamma_2}{2}+\sin^2\frac{\Gamma_2}{2})[|p_{ccw}(x,y)|^2+|p_{cw}(x,y)|^2 -\exp(-i\Gamma_1)p_{ccw}(x,y)p^{*}_{cw}(x,y)-\exp(i\Gamma_1)p_{cw}(x,y)p^{*}_{ccw}(x,y)]. \quad (20)$$

Although PSFs are not affected by Γ_2, we didn't omit

the terms $(\cos^2\frac{\Gamma_2}{2}+\sin^2\frac{\Gamma_2}{2})$ in Eqs. (17) and (20). Because we used the wave plate 2 to obtain sine term, it is desirable to obtain cosine term without the change of the component devices of the system. Then, in the case in which $\Gamma_1 = 0$ (which means that wave plate 1 is removed in the MTI) and $\Gamma_2 = \pi/2$, from Eqs. (17) and (20), we obtain cosine component.

$$h_r(x,y) = \frac{1}{2}\left[h_{45}(x,y;0,\frac{\pi}{2}) - h_{-45}(x,y;0,\frac{\pi}{2})\right]$$
$$= |p_{cw}(x,y)p_{ccw}(x,y)|\cos\phi(x,y). \quad (21)$$

From Eq. (21), we see that we can obtain the cosine function using two intensity patterns obtained by rotating a linear polarizer by 45 degrees and -45 degrees, respectively, with respect to x axis in the MTI with only wave plate 2. We can obtain the complex hologram without bias and conjugate image by the electronic combination of Eqs. (13) and (21). Table 1 shows the PSFs by the combination of the azimuth angle of a linear polarizer and the phase retardation of wave plate 2 in the MTI. We see that the complex hologram without bias and without conjugate image is obtained by combining four PSFs in Table 1 electronically, and Fig. 2 shows the optimized MTI with one wave plate.

III. PHASE ERROR ANALYSIS

The main potential sources of error in the optimized MTI are imperfections of the polarization elements and azimuth angle error of the polarization elements. We shall analyze the effects of these potential error sources one by one.

In Fig. 2, the Jones matrix of output beam in the output plane is given by

TABLE 1. Intensity patterns by combination of a wave plate and a linear polarizer.

Azimuth angle of a linear polarizer (degree)	Phase retardation of a wave plate	PSF
0	$\Gamma_2 = \frac{\pi}{2}$	$\frac{1}{2}[1-\sin\phi(x,y)]$
	$\Gamma_2 = -\frac{\pi}{2}$	$\frac{1}{2}[1+\sin\phi(x,y)]$
45	$\Gamma_2 = \frac{\pi}{2}$	$\frac{1}{2}[1+\cos\phi(x,y)]$
-45	$\Gamma_2 = \frac{\pi}{2}$	$\frac{1}{2}[1-\cos\phi(x,y)]$

$$E_{out} = A(\varphi_2)W(\varphi_1)E_{in}, \quad (22)$$

where E_{in} represents input optical wave, and $A(\varphi_2)$ and $W(\varphi_1)$ represent Jones matrices of a linear polarizer and a wave plate, respectively. The Jones matrices of polarization components are given by, respectively,

$$E_{in} = \begin{pmatrix} p_{ccw} \\ p_{cw} \end{pmatrix} = \begin{pmatrix} b\exp(-i\theta_{ccw}) \\ a\exp(-i\theta_{cw}) \end{pmatrix}, \quad (23)$$

$$A(\varphi_2) = \begin{pmatrix} \cos^2\varphi_2 & 1/2\sin 2\varphi_2 \\ 1/2\sin 2\varphi_2 & \sin^2\varphi_2 \end{pmatrix}, \quad (24)$$

$$W(\varphi_1) = \begin{pmatrix} 2i\sin^2\varphi_1\sin\frac{\Gamma}{2}+\exp(-i\frac{\Gamma}{2}) & -i\sin 2\varphi_1\sin\frac{\Gamma}{2} \\ -i\sin 2\varphi_1\sin\frac{\Gamma}{2} & -2i\sin^2\varphi_1\sin\frac{\Gamma}{2}+\exp(i\frac{\Gamma}{2}) \end{pmatrix}, \quad (25)$$

where $W(\varphi_1)$ represents the Jones matrix for $\lambda/4$ plate. φ_2 and φ_1 represent the azimuth angle of a linear polarizer and a wave plate, respectively. Γ represents the phase retardation of a wave plate. The intensity of Eq. (22) is given by

$$I = |E_{out}|^2. \quad (26)$$

A. Phase error due to imperfections of a wave plate

We shall deal mainly with the errors that are introduced by imperfections in $\lambda/4$ plate. In this case, we assume that the azimuth angle error of wave plate is zero. The phase error introduced by imperfections in $\lambda/4$ plate can be obtained from four intensity patterns as follows.

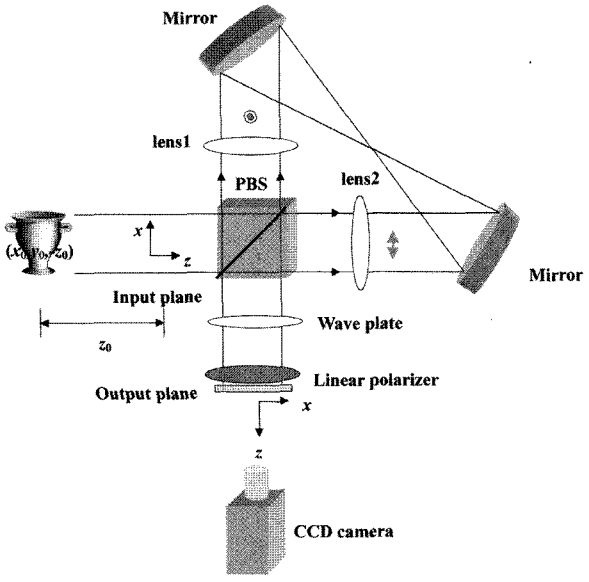

FIG. 2. Optimized MTI.

From Eq. (26), intensity for $\varphi_1 = \pi/4$ and $\varphi_2 = 0$ is given by

$$I_1 = \frac{1}{2}a^2(1-\cos\Gamma) + \frac{1}{2}b^2(1+\cos\Gamma) - ab\sin\phi\sin\Gamma . \quad (27)$$

By the same method, intensities for $\varphi_1 = -\pi/4$ and $\varphi_2 = 0$, $\varphi_1 = \pi/4$ and $\varphi_2 = \pi/4$, and $\varphi_1 = \pi/4$ and $\varphi_2 = -\pi/4$ are given by, respectively,

$$I_2 = \frac{1}{2}a^2(1-\cos\Gamma) + \frac{1}{2}b^2(1+\cos\Gamma) + ab\sin\phi\sin\Gamma , \quad (28)$$

$$I_3 = \frac{1}{2}a^2 + \frac{1}{2}b^2 + ab\cos\phi , \quad (29)$$

$$I_4 = \frac{1}{2}a^2 + \frac{1}{2}b^2 - ab\cos\phi . \quad (30)$$

From Eqs. (27)~(30), the phase difference ϕ' of optical waves p_{cw} and p_{ccw} is given by

$$\tan\phi' = \frac{I_2 - I_1}{I_3 - I_4} = \tan\phi\sin\Gamma , \quad (31)$$

where ϕ' includes the error introduced by a wave plate. For a nonideal $\lambda/4$ plate, we have

$$\Gamma = \frac{\pi}{2} + \alpha , \quad (32)$$

where α is the error in the relative retardation introduced by plate. Substituting Eq. (32) into Eq. (31), we obtain

$$\tan\phi' = \tan\phi\cos\alpha . \quad (33)$$

Since

$$\tan\phi' = \tan(\phi + \Delta\phi) \approx \tan\phi + \Delta\phi\sec^2\phi , \quad (34)$$

we can calculate phase error from Eqs. (33) and (34) as follows:

$$\Delta\phi = -\frac{1}{4}\alpha^2\sin(2\phi) . \quad (35)$$

Figure 3 shows the phase error of Eq. (35). Here phase tolerance of the $\lambda/4$ plate was set to $\lambda/300$ because the retardation error of the commercially available wave plate is $\pm\lambda/300$ at 20℃±1℃. In Fig. 3, phase error is minimum at $\pi/4$ and phase error is maximum at $-\pi/4$, and phase error is zero at 0.

B. Phase error due to the azimuth angle error of a wave plate

In this section, we shall deal with the phase error that is introduced by the azimuth angle error in the $\pi/4$ plate. In this case, we assume that a wave plate is ideal and the azimuth angle errors of all polarization elements are zero except a wave plate. For $\varphi_1 = \pi/4$ and $\varphi_1 = -\pi/4$, we assume that azimuths of a wave plate including error are $\varphi_1 = \pi/4+\beta_1$ and $\varphi_1 = -\pi/4+\beta_2$, and β_1 and β_2 represent the azimuth angle errors of a wave plate.

From Eq. (26), intensities for $\varphi_1 = \pi/4+\beta_1$ and $\varphi_2 = 0$, $\varphi_1 = -\pi/4+\beta_2$ and $\varphi_2 = 0$, $\varphi_1 = \pi/4+\beta_1$ and $\varphi_2 = \pi/4$, $\varphi_1 = \pi/4+\beta_1$ and $\varphi_2 = -\pi/4$ are given by, respectively,

$$I_1 = \frac{1}{2}a^2 + b^2(\frac{1}{2} + 2\beta_1^2) - ab(2\beta_1\cos\phi + \sin\phi) , \quad (36)$$

$$I_2 = \frac{1}{2}a^2 + b^2(\frac{1}{2} + 2\beta_2^2) - ab(2\beta_2\cos\phi - \sin\phi) , \quad (37)$$

$$I_3 = \frac{1}{2}a^2(1+2\beta_1+2\beta_1^2) + \frac{1}{2}b^2(1-2\beta_1+2\beta_1^2) + ab(\cos\phi - 2\beta_1\sin\phi) , \quad (38)$$

$$I_4 = \frac{1}{2}a^2(1-2\beta_1+2\beta_1^2) + \frac{1}{2}b^2(1+2\beta_1+2\beta_1^2) - ab(\cos\phi - 2\beta_1\sin\phi) . \quad (39)$$

From Eqs. (36)~(39), the phase difference ϕ' of optical waves p_{cw} and p_{ccw} is given by

$$\tan\phi' = \frac{I_2 - I_1}{I_3 - I_4} = \frac{\frac{b}{a}(\beta_2^2 - \beta_1^2) - (\beta_2 - \beta_1)\cos\phi + \sin\phi}{2\beta_1\cot 2\beta + \cos\phi - 2\beta_1\sin\phi}$$
$$\approx \tan\phi + \frac{1 + \sin^2\phi - 2\cot 2\beta\sin\phi}{\cos^2\phi}\beta_1 - \beta_2 , \quad (40)$$

where $\cot 2\beta = (b^2 - a^2)/2ab$. From Eqs. (34) and (40), we obtain the phase error as

$$\Delta\phi = (1 + \sin^2\phi - 2\cot 2\beta\sin\phi)\beta_1 - \beta_2\cos^2\phi . \quad (41)$$

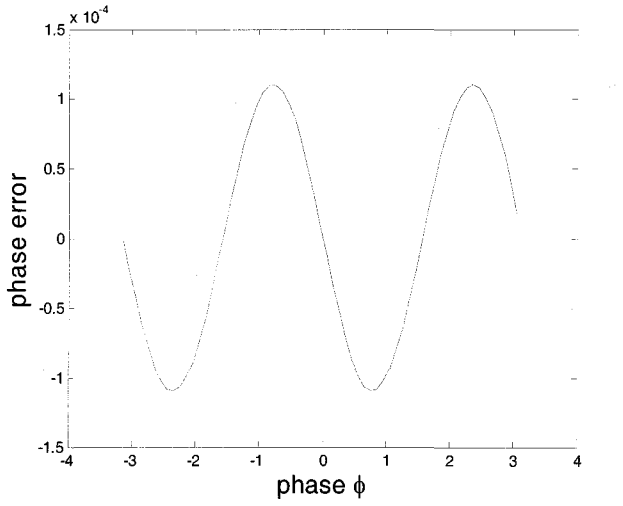

FIG. 3. Phase error due to the imperfections of wave plate

Figure 4 shows the phase error of Eq. (41). Here we suggested $\cot 2\beta = 0$. In solid line, azimuth angle errors of $\pi/4$ plate were set to $\beta_1 = 2\pi/300$ and $\beta_2 = 2\pi/300$. In dashed line, azimuth angle errors of $\lambda/4$ plate were set to $\beta_1 = 2\pi/300$ and $\beta_2 = 0$. In Fig. 4, phase error becomes minimum at 0 and phase error becomes maximum at about $\pm\pi/2$.

C. Phase error due to the azimuth angle error of a linear polarizer

We shall deal with the phase error that is introduced by the azimuth angle error in the linear polarizer. In this case, we assume that a linear polarizer is ideal and the azimuth angle errors of all polarization elements are zero except a linear polarizer. For $\varphi_2 = 0$, $\varphi_2 = \pi/4$ and $\varphi_2 = -\pi/4$, we assume that azimuths of a linear polarizer including error are $\varphi_2 = 0+\gamma_1$, $\varphi_2 = \pi/4+\gamma_2$ and $\varphi_2 = -\pi/4+\gamma_3$, respectively, and γ_1, γ_2 and γ_3 represent the azimuth angle errors of a linear polarizer.

From Eq. (26), intensities for $\varphi_1 = \pi/4$ and $\varphi_2 = 0+\gamma_1$, $\varphi_1 = -\pi/4$ and $\varphi_2 = 0+\gamma_1$, $\varphi_1 = \pi/4$ and $\varphi_2 = \pi/4+\gamma_2$, $\varphi_1 = \pi/4$ and $\varphi_2 = -\pi/4+\gamma_3$ are given by, respectively,

$$I_1 = \frac{1}{2}(a^2+b^2) - ab(2\gamma_1\cos\phi - \sin\phi), \tag{42}$$

$$I_2 = \frac{1}{2}(a^2+b^2) + ab(2\gamma_1\cos\phi + \sin\phi), \tag{43}$$

$$I_3 = \frac{1}{2}(a^2+b^2) + ab(\cos\phi + 2\gamma_2\sin\phi), \tag{44}$$

$$I_4 = \frac{1}{2}(a^2+b^2) - ab(\cos\phi + 2\gamma_3\sin\phi). \tag{45}$$

From Eqs. (42)~(45), the phase difference ϕ' of optical waves p_{cw} and p_{ccw} is given by

$$\tan\phi'(x,y) = \frac{I_2 - I_1}{I_3 - I_4} = \frac{\sin\phi}{[\cos\phi + (\gamma_2+\gamma_3)\sin\phi]} \approx \tan\phi - \tan^2\phi(\gamma_2+\gamma_3). \tag{46}$$

From Eq. (34) and Eq. (46), we obtain the phase error as

$$\Delta\phi = -(\gamma_2+\gamma_3)\sin^2\phi. \tag{47}$$

Figure 5 shows the phase error of Eq. (47). In solid line, azimuth angle errors of $\lambda/4$ plate were set to $\gamma_2 = 2\pi/300$ and $\gamma_3 = 2\pi/300$. In dashed line, azimuth angle errors of $\lambda/4$ plate were set to $\gamma_2 = 2\pi/300$ and $\gamma_3 = 0$. In Fig. 5, phase error becomes minimum at 0 and phase error becomes maximum at about $\pm\pi/2$.

Then, total phase error by polarization components is written by

$$\Delta\phi = -\frac{1}{4}\alpha^2\sin(2\phi) + (1+\sin^2\phi - 2\cot 2\beta\sin\phi)\beta_1 - \beta_2\cos^2\phi - (\gamma_2+\gamma_3)\sin^2\phi. \tag{48}$$

If $a = b$, then $\cot 2\beta = 0$. In this case, total phase error is given by

$$\Delta\phi = -\frac{1}{4}\alpha^2\sin(2\phi) + (1+\sin^2\phi)\beta_1 - \beta_2\cos^2\phi - (\gamma_2+\gamma_3)\sin^2\phi. \tag{49}$$

Figure 6 shows total phase error of Eq. (49). In solid line, azimuth angle errors of $\lambda/4$ plate and a linear polarizer were set to $\beta_1 = 2\pi/300$, $\beta_2 = 2\pi/300$ and $\gamma_2 = 2\pi/300$, $\gamma_3 = 2\pi/300$, respectively. In dashed line, azimuth angle errors of $\lambda/4$ plate were and a linear polarizer set to $\beta_1 = 2\pi/300$, $\beta_2 = 0$ and $\gamma_2 = 2\pi/300$,

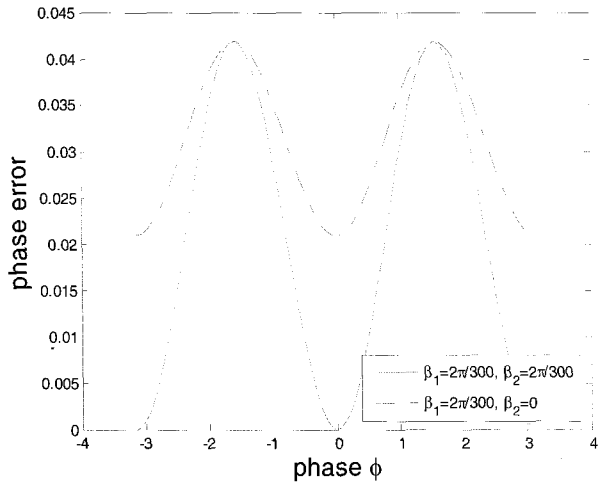

FIG. 4. Phase error due to the azimuth angle error of a wave plate

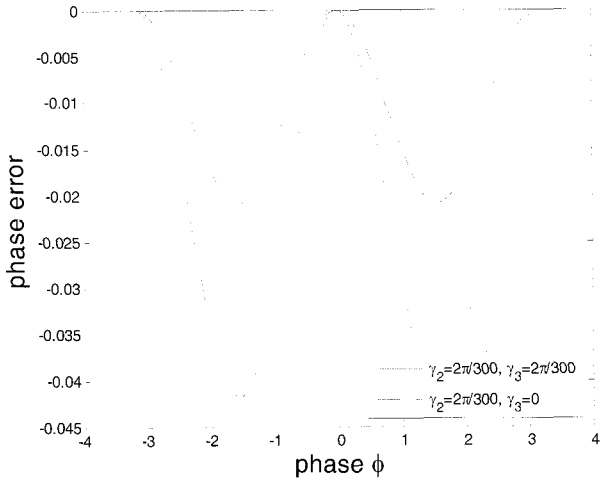

FIG. 5. Phase error due to the azimuth angle error of a linear polarizer

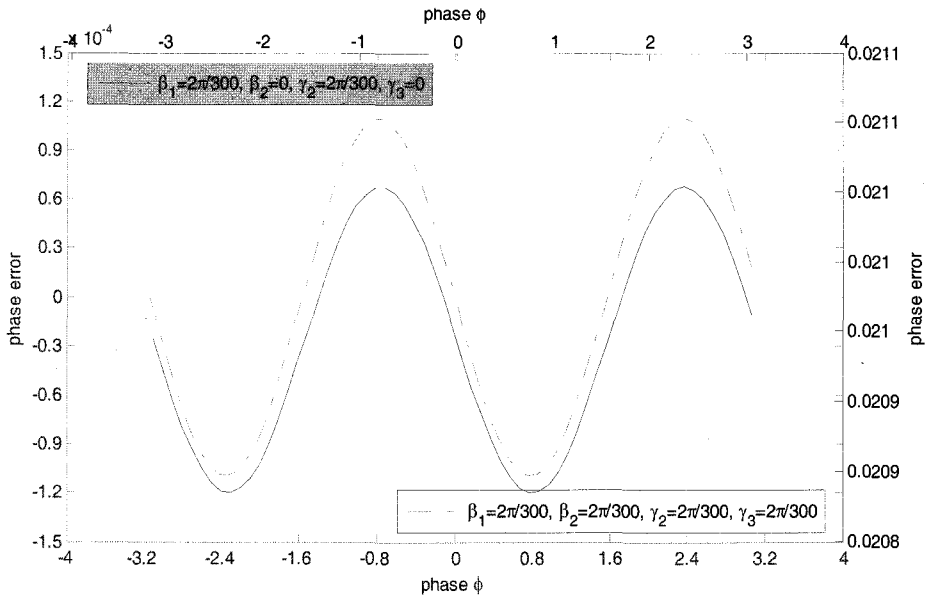

FIG. 6. Total phase error by polarization components

$\gamma_3 = 0$. In Fig. 6, phase error is minimum at $\pi/4$ and phase error is maximum at $-\pi/4$.

In the extraction of phase term using the combination of polarization components, the phase error occurs. As shown in Fig. 3, the retardation error of the commercially available wave plate makes the second-order error very small. Accordingly, we see that phase error in the optimized MTI is mainly due to the azimuth angle errors of the polarization components.

IV. CONCLUSIONS

We need two operation modes to obtain the complex hologram without bias and the conjugate image in the MTI. To solve the problem, we proposed the optimized MTI with one wave plate, which can obtain cosine and sine functions by the combination of one wave plate and one linear polarizer.

In the extraction of phase term using the combination of polarization components, the phase error occurs, and we analyzed such potential phase errors in the optimized MTI. The retardation error of the commercially available wave plate makes the second-order error very small. Accordingly, phase error in the optimized MTI is mainly due to the azimuth angle errors of the polarization components. The azimuth angle errors can be minimized by using a computer-controlled phase-shifting apparatus, which can accurately control the rotating angle of the polarization components.

*Corresponding author : sgkim@office.hoseo.ac.kr

REFERENCES

[1] W. Lukosz, "Properties of linear low-pass filters for nonnegative signals," *J. Opt. Soc. Am.*, vol. 52, pp. 827-829, 1962.

[2] A. W. Lohmann and W. T. Rhodes, "Two-pupil synthesis of optical transfer function," *Appl. Opt.*, vol. 17, pp. 1141-1151, 1978.

[3] D. Goerlitz and F. Lanzl, "Methods of zero-order non-coherent filtering," *Opt. Commun.*, vol. 20, pp. 68-72, 1977.

[4] A. W. Lohmann, "Incoherent optical processing of complex data," *Appl. Opt.*, vol. 16, pp. 261-263, 1977.

[5] W. Stoner, "Incoherent optical processing via spatially offset pupil masks," *Appl. Opt.*, vol. 17, pp. 2454-2466, 1978.

[6] W. T. Rhodes, "Bipolar pointspread function synthesis by phase switching," *Appl. Opt.*, vol. 16, pp. 265-267, 1977.

[7] S.-G. Kim, B. Lee, and E.-S. Kim, "Removal of bias and the conjugate image in incoherent on-axis triangular holography and real-time reconstruction of the complex hologram," *Appl. Opt.*, vol. 36, pp. 4784-4791, 1997.

[8] S.-G. Kim, B. Lee, E.-S. Kim, and C.-W. Yi, "Resolution analysis of incoherent triangular holography," *Appl. Opt.*, vol. 40, pp. 4672-4678, 2001.

[9] G. Cochran, "New method of making Fresnel transforms with incoherent light," *J. Opt. Soc. Am.*, vol. 56, pp. 1513-1517, 1966.

[10] W. H. Stevenson, "Optical frequency shifting by means of a rotating diffraction grating," *Appl. Opt.*, vol. 9, pp. 649-652, 1970.

[11] R. N. Shagam and J. C. Wyant, "Optical frequency shifter for heterodyne interferometers using multiple rotating polarization retards," *Appl. Opt.*, vol. 17, pp. 3034-3035, 1978.

[12] M. P. Kothiyal and C. Delisle, "Polarization component phase shifters in phase shifting interferometry: error analysis," *Optica Acta*, vol. 33, pp. 787-793, 1986.
[13] H. Z. Hu, "Polarization heterodyne interferometry using a simple rotating analyzer. 1: theory and error analysis," *Appl. Opt.*, vol. 22, pp. 2052-2056, 1983.
[14] A. Yariv and P. Yeh, *Optical Waves in Crystals* (Wiley, New York, 1984) Chap. 5.
[15] Y. R. Song, M. H. Lee, and S. S. Lee, "A modulated Gaussian pupil derived diffraction inverse problem approach and the characteristics of the OTF of the system," *Hankook Kwanghak Hoeji*, vol. 8, pp. 95-98, 1997.